DOI: 10.1111/tgis.12590

RESEARCH ARTICLE

Transactions in GIS WILEY

Similarity measurement on human mobility data with spatially weighted structural similarity index (SpSSIM)

Chanwoo Jin[1,2,3] | Atsushi Nara[1,3] | Jiue-An Yang[4] | Ming-Hsiang Tsou[1,3]

[1]Department of Geography, San Diego State University, San Diego, California, USA

[2]Department of Geography, University of California Santa Barbara, Santa Barbara, California, USA

[3]Center for Human Dynamics in the Mobile Age, San Diego, California, USA

[4]Calit2/Qualcomm Institute, University of California San Diego, La Jolla, California, USA

Correspondence
Atsushi Nara, Department of Geography, San Diego State University, San Diego, CA 92182, USA.
Email: anara@sdsu.edu

Funding information
National Science Foundation, Grant/Award Number: 1634641

Abstract

Understanding diverse characteristics of human mobility provides profound knowledge of urban dynamics and complexity. Human movements are recorded in a variety of data sources and each describes unique mobility characteristics. Revealing similarity and difference in mobility data sources facilitates grasping comprehensive human mobility patterns. This study introduces a new method to measure similarities on two origin–destination (OD) matrices by spatially extending an image-assessment tool, the structural similarity index (SSIM). The new measurement, spatially weighted SSIM (SpSSIM), utilizes weight matrices to overcome the SSIM sensitivity issue due to the ordering of OD pairs by explicitly defining spatial adjacency. To evaluate SpSSIM, we compared performances between SSIM and SpSSIM with resampling the orders of OD pairs and conducted bootstrapping to test the statistical significance of SpSSIM. As a case study, we compared OD matrices generated from three data sources in San Diego County, CA: U.S. Census-based Longitudinal Employer–Household Dynamics Origin–Destination employment statistics, Twitter, and Instagram. The case study demonstrated that SpSSIM was able to capture similarities of mobility patterns between datasets that varied by distance. Some regions showed local dissimilarity while the global index indicated they were similar. The results enhance the understanding of complex mobility patterns from various datasets, including social media.

1 | INTRODUCTION

Urban dynamics are built up based on diverse types of human movements, including migration, commuting, and leisure activities, and hence the study of human mobility is essential for understanding complex urban systems (Dodge, Weibel, Ahearn, Buchin, & Miller, 2016; Miller & Shaw, 2015). To examine human mobility and urban dynamics, various forms of data sources exist; for instance, census surveys, activity diaries, call detail records (CDRs) from cellphones, GPS points, and new media data. Among these, researchers have recently adopted social media data, which has produced a massive amount of publicly available individual-scale time-stamped geo-referenced data, for discovering unrevealed travel patterns and activities. For example, finding major human flows (Gao, Li, Wang, Jeong, & Soltani, 2018; Poon & Pandit, 1996; Xu, Li, Shi, Zhang, & Jiang, 2015) can support decisions across multiple fields, including public health, epidemiology, and disaster response (Martín, Li, & Cutter, 2017; Nara, Yang, Machiani, & Tsou, 2017; Panigutti, Tizzoni, Bajardi, Smoreda, & Colizza, 2017; Wesolowski et al., 2015). While previous studies have often examined and analyzed spatial distributions of movements, less research has focused on measuring similarities and differences between multiple data sources (Gao et al., 2018). Each data source has its own unique characteristics to describe human mobility due to diversities in survey participants or platform users who provide their mobility data, and methodologies to collect, manage, and publish geo-referenced data. For instance, in the case of social media data demographic characteristics, Instagram use is more popular among female and younger populations than Twitter (Table 1), the variations of which may produce significant differences in mobility patterns and play a significant role in shaping the complexity of human mobility.

Therefore, it is crucial to understand the capabilities and limitations of each data source for describing human mobility. This can further help in grasping comprehensive human mobility patterns, where multiple mobility data sources complement one another in explaining different types of human movements. There have been attempts to develop new methodologies to measure similarities between mobility patterns from diverse sources (Xia, Wang, Zhang, Kim, & Bae, 2011; Yuan & Raubal, 2014), and to address those demographic biases on multiple social media data (Crooks et al., 2015; Gao et al., 2017). However, effectively and quantitatively measuring mobility similarities from multiple data sources continues to be a research challenge.

To address this research gap, the present article proposes a new method, the spatially weighted structural similarity index (SpSSIM), to measure the similarity of origin–destination (OD) flow matrices to compare mobility patterns from multiple data sources. SpSSIM adopted the structural similarity index (SSIM), an image quality assessment technique to measure the similarity between two images (Wang, Bovik, Sheikh, & Simmoncelli, 2004). SSIM has been applied to measure the similarity of human mobility by mapping the OD matrices into arrays of image values; however, previous works do not consider the spatial configuration of flows on the OD matrices. We extended SSIM by

TABLE 1 Demographic characteristics of Instagram and Twitter users in the USA (Greenwood, Perrin, & Duggan, 2016)[a]

		Instagram	Twitter
All online adults		32	24
Gender	Men	26	24
	Women	38	25
Age	18–29	59	36
	30–49	33	23
	50–64	18	21
	65+	8	10

[a]% of online adults who use social media.

incorporating spatial adjacency by utilizing a series of spatial weight matrices. A key advantage of SpSSIM is that local similarities can be properly measured and investigated.

While SSIM utilizes a square moving window to calculate the similarity of images or matrices, SpSSIM employs a geographically defined range with spatial weights. This enables SpSSIM to calculate similarities of flows in a certain geographic boundary. As our case study, we compared each pair of OD matrices of human daily mobility extracted from three mobility data sources: U.S. Census-based Longitudinal Employer–Household Dynamics Origin–Destination employment statistics (LODES), Twitter, and Instagram, and aggregated at the subregional areas (SRAs) scale in San Diego County, CA. Two geo-referenced social media data, Twitter and Instagram, were collected via publicly available application programming interfaces (APIs) in 2015. The case study demonstrated the capability of SpSSIM to measure the mobility similarities between each data source and to provide underlying knowledge of human mobility extracted from social media data, which can ultimately facilitate the understanding of the complexities of human mobility. The remainder of this article is organized as follows. Section 2 describes related works on measuring the similarity of human mobility and studying human mobility with social media data. Section 3 introduces the SpSSIM methodology and Section 4 describes the data used in this study. Section 5 details the results of comparative experiments between SSIM and SpSSIM and the interpretation of SpSSIM values, with a case study of San Diego County, CA. Finally, Section 6 discusses the implications of the results and our conclusions, along with suggested future work.

2 | RELATED WORK

2.1 | Methodological approaches for quantifying similarity of mobility

Methodological approaches to characterize and compare mobility patterns have been, in essence, quantifying similarity in mobility data, which can identify major trends in movements and allow the comparison of trends from diverse data sources. As a traditional approach, dominant flow analysis (Nystuen & Dacey, 1961) counted the amount of flow and detected major trends of human mobility, such as trading (Smith, 1970; Xu et al., 2015) and tourist travel (Pearce, 1996). Another approach was to employ principal component analysis (PCA) to identify the centers of mobility networks (Garrison & Marble, 1964). Components derived from PCA represent the similarity of regions regarding the amount of flow (Poon & Pandit, 1996). For example, Clayton (1977) categorized U.S. states in terms of the similarity of origins and the numbers of inter-state immigrants. More recently, Gao et al. (2018) employed spatial scan statistics (Kulldorff, 1997) to compare major patterns of taxi trips in the morning and afternoon in New York City and county-to-county migration flows between age groups in the U.S. by clustering origins and destinations. While these methodological approaches have been effective in summarizing mobility patterns with a few major trends, the number of clusters was potentially arbitrary and the comparison was limited to detected clusters (Salvador & Chan, 2004). In other words, the similarities measured by clusters can be sensitive to the number of clusters and clustering methods.

Various methodologies have been explored to calculate the similarity between mobility data, which are often treated as trajectories (i.e., two sets of temporally sequenced location points). Common trajectory similarity measurements calculate distances between points on each trajectory. For example, Euclidian distance has been widely used to measure geographic gaps between two points from each trajectory (Zheng & Zhou, 2011). Meanwhile, the Levenshtein distance, or edit distance, developed from informatics to measure the distance between two strings has also been applied to geographic trajectories by matching each of their intermediate points and calculating the differences (Yuan & Nara, 2015; Yuan & Raubal, 2014). These approaches provide similarity measurements of individual sequential movements. More recently, Behara, Bhaskar, and Chung (2018) proposed a mean normalized Levenshtein distance for OD matrices (MNLdOD) by applying the Levenshtein distance to measure the similarity of two OD matrices. This measurement compares the descending order of destinations by the normalized flow

volume from each origin (i.e., a row of OD matrices) as strings, and calculates the similarity row by row to capture differences in the order of destination choices from the same origin. Since MNLdOD employs the orders by flow volumes rather than the actual amounts of flow, it is limited in fully incorporating flow volume variations in its similarity index.

2.2 | Human mobility and social media

Human mobility has been a long-discussed issue in social and geographic sciences, and complex mobility dynamics and behaviors have been studied in a variety of applications, including migration, travel, and evacuation (Cresswell, 2012; Noulas, Scellato, Lambiotte, Pontil, & Mascolo, 2012). Focusing on the daily human mobility, fundamental activities of human living such as commuting, shopping, and leisure trips often accompany movements, which further contribute to form complex urban dynamics through human–human and human–environment interactions in space and time (Huang & Wong, 2016; Sun, Fan, Li, & Zipf, 2015; Wu, Zhi, Sui, & Liu, 2014). Thus, investigating human mobility is key to comprehending complex urban systems; yet it has been challenging (Larsen, Urry, & Axhusen, 2006; Yuan & Raubal, 2014), especially since traditional data collection methods (e.g., census surveys and travel diaries) were limited in observing and recording human mobility at full scale due to their high cost (Miller & Shaw, 2015). Nowadays, recent advancements in and adaptations of mobile information and communication technologies (mICTs) and location-aware technologies (LATs) have enabled the recording of human mobility via mobile devices. This larger and finer-scale spatiotemporal data can fulfill the investigation of daily human mobility and reveal undiscovered patterns not captured in the data collected through traditional methods (Hawelka et al., 2014; Liu, Kang, Gao, Xiao, & Tian, 2012; Wu et al., 2014).

Social media is one of the data sources that can capture human mobility by taking advantage of mICTs and LATs. Recent studies have explored the potential of social media data to reconstruct individual trajectories and describe dynamic human movement behaviors in detail (Nara et al., 2017). For example, travel patterns and behaviors have been studied using check-in data to detect hotspots and unusual visiting places (Sun et al., 2015), and geo-tagged Twitter posts to estimate the volume of country-to-country flows (Hawelka et al., 2014). Geo-tagged social media posts have been applied to investigate human mobility and evacuation behavior during disastrous events (Li, Wang, Emrich, & Guo, 2018; Martín et al., 2017; Wang & Taylor, 2014). Despite the usefulness of social media data to investigate human and urban dynamics, they are known to be biased by the unevenness of demographic, geographic, and temporal distributions. Furthermore, since each social media platform has its own unique usage and demographics, human mobility patterns extracted from social media data potentially differ by platform; however, few studies have investigated the similarity and difference in human mobility by social media platform.

To solve the bias of a single social media data source, some studies have integrated multiple social media data sources with other spatial and aspatial data to gain profound knowledge in human activities and urban contexts. For instance, Gao et al. (2017) synthesized multiple data sources from Flickr, Instagram, Twitter, Travel Blogs, and Wikipedia to extract semantics and identify cognitive regions based on a belief that each source represented different user groups. They assumed that Flicker was more tourism-oriented than other social media such as Twitter and Instagram, which showed daily activities, news, and visited places. Crooks et al. (2015) utilized open-source crowdsourcing datasets ranging from GPS tracks and Foursquare to Twitter, Flickr, and weblogs to demonstrate how social media, trajectory, and traffic data could be analyzed to capture the evolving nature of a city's form and function. They argued that each data source represented part of a dynamic and complex urban function. These approaches highlighted the importance of integrating multiple data sources to gain deeper insights into urban dynamics. Despite the importance and necessity of data integration in mobility studies, it has been utilized less due to our limited understanding of the capabilities and limitations of each data source and their similarities and differences.

3 | METHODOLOGY

This article proposes a novel index, SpSSIM, to measure the similarity of two OD flow matrices to compare mobility patterns. Our method adopted the concept of the SSIM, which originally assessed image quality by comparing local patterns of image structure. We extended SSIM spatially by utilizing a series of spatial weight matrices that define the range of a neighborhood geographically. The following subsections demonstrate the SSIM algorithm, the process of spatial extension, and verification of SpSSIM.

3.1 | Spatially weighted structural similarity index

Wang et al. (2004) developed SSIM to measure the similarity between two images for assessing the quality of copied or generated images from an original image. As the human visual system is familiar with the overall arrangement of images rather than single values of cells to compare images, SSIM consideres the arrangement of image values by quantifying the local patterns of pixel intensities consisting of three components—luminance, contrast, and structure—with a moving window. SSIM calculates image similarity between two images X and Y as expressed in Equation (1):

$$\mathrm{SSIM}(x,y)=[l(x,y)^{\alpha}\cdot c(x,y)^{\beta}\cdot s(x,y)^{\gamma}]$$

$$l(x,y)=\frac{2\mu_x\mu_y+C_1}{\mu_x^2+\mu_y^2+C_1},\ c(x,y)=\frac{2\sigma_x\sigma_y+C_2}{\sigma_x^2+\sigma_y^2+C_2},\ s(x,y)=\frac{\sigma_{xy}+C_3}{\sigma_x\sigma_y+C_3} \tag{1}$$

where $l(x,y)^{\alpha}$, $c(x,y)^{\beta}$, and $s(x,y)^{\gamma}$ represent the three components of luminance, contrast, and structure, respectively. x and y denote black/white color values of pixels (0 to 255) in images X and Y. μ, σ^2, and σ_{xy} refer to mean, variance, and covariance, respectively. C_1, C_2, and C_3 are constants that enforce SSIM to be less than 1. Therefore, the value of SSIM equals 1 when two images are exactly the same, and it gets close to 0 when they are less similar. When we regard the importance of each component as identical ($\alpha=\beta=\gamma=1$), and C_3 is equal to $C_2/2$, Equation (1) can be simplified to:

$$\mathrm{SSIM}(x,y)=\frac{(2\mu_x\mu_y+C_1)(2\sigma_{xy}+C_2)}{(\mu_x^2+\mu_y^2+C_1)(\sigma_x^2+\sigma_y^2+C_2)} \tag{2}$$

Once SSIM is calculated in a window, it moves to the next cells and computes SSIM from the last cell of images. Then, the overall similarity of images X and Y is represented by the mean of local SSIM values, where M denotes the total number of local windows:

$$\mathrm{MSSIM}(X,Y)=\frac{1}{M}\sum_{j=1}^{M}\mathrm{SSIM}(x_j,y_j) \tag{3}$$

SSIM has been widely utilized to assess the quality of images and to evaluate the performance of image processing due to its simplicity and accuracy (Brunet, Vrscay, & Wang, 2012). The index has recently been employed to compare movements because the amount of flow in OD matrices can be considered as values of images (Djukic, 2014; Pollard, Taylor, & Vuren, 2013). For example, Djukic (2014) used SSIM with a square window to evaluate the estimation of OD demands in traffic flows (Figure 1) since traditional statistics such as the mean square error are limited to considering the spatial correlation between OD pairs. Yet, SSIM is still problematic in terms of the sensitivity of OD pairs ordering because the order in a matrix is not always arranged by spatial contiguity or distance. For example, the contiguous cells in an OD matrix can be far from each other in real space when the order is based

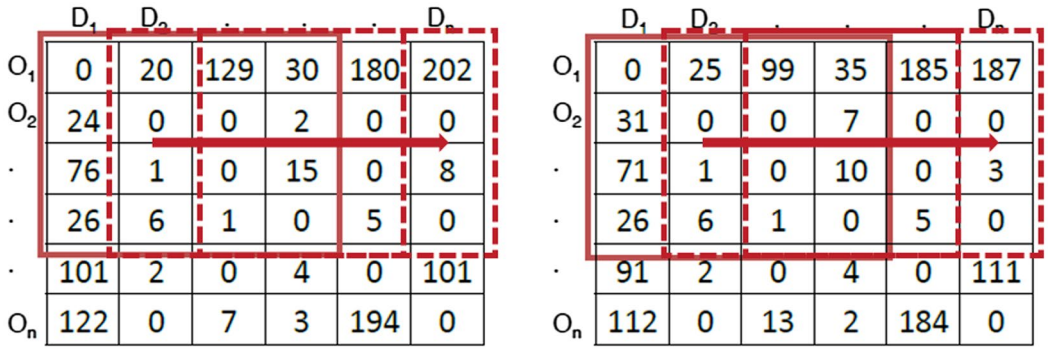

FIGURE 1 Comparison of two OD matrices using SSIM (Pollard et al., 2013)

on the size of the population or is randomly distributed. In this case, a square window is limited to filtering out the spatial correlation between OD pairs because contiguous cells are not spatially adjacent. Moreover, the same values of OD matrices with different orders result in different SSIM values. To solve the problem, Djukic (2014) suggested finding the best way to represent spatial dependency of OD pairs by testing various window sizes, and Behara, Bhaskar, and Chung (2017) reordered OD pairs to group to the upper level and calculated SSIM within the new level; however, selecting the optimal window size and the optimal order of OD pairs remains challenging.

To overcome the SSIM ordering issue to compare OD matrices, SpSSIM (Equation 4) utilizes a series of spatial weight matrices instead of the moving window of SSIM. The range of locality is defined by multiplying a spatial weight matrix with an OD matrix using the Hadamard product (Equation 5). The spatial weight matrix consists of 0 and 1, where flows (f_{ij}) in the distance range (d_{ij}) have a weight value of 1 (Equation 6). In other words, SpSSIM computes a similarity between two OD matrices only in a specific geographic range by blocking values from outside the range, multiplying the value by 0 (Figure 2). As a result, SpSSIM will have a value between 0 and 1 and be close to 1 when two matrices are similar.

$$\mathrm{SpSSIM}(x,y,w)=\frac{\left(2\mu_{wx}\mu_{wy}+C_1\right)\left(2\sigma_{wx,wy}+C_2\right)}{\left(\mu_{wx}^2+\mu_{wy}^2+C_1\right)\left(\sigma_{wx}^2+\sigma_{wy}^2+C_2\right)} \tag{4}$$

$$WF=W\circ F=\begin{bmatrix} w_{11} & \cdots & w_{1j} \\ \vdots & \ddots & \vdots \\ w_{i1} & \cdots & w_{ij} \end{bmatrix}\circ\begin{bmatrix} f_{11} & \cdots & f_{1j} \\ \vdots & \ddots & \vdots \\ f_{i1} & \cdots & f_{ij} \end{bmatrix}=\begin{bmatrix} w_{11}f_{11} & \cdots & w_{1j}f_{1j} \\ \vdots & \ddots & \vdots \\ w_{i1}f_{i1} & \cdots & w_{ij}f_{ij} \end{bmatrix} \tag{5}$$

$$w_{ij}^{D_{\max}^{\min}}=\begin{cases} 1, D_{\min}\le d_{ij}<D_{\max} \\ 0, \text{otherwise} \end{cases} \tag{6}$$

For the global similarity between two OD matrices, a series of spatial weight matrices is required to encompass the whole study area (Equation 7). For instance, if the first spatial weight matrix takes the value of 1 when the distance between two regions is less than 10 km (bin 1), then flows in the range 0–10 km are included for a local SpSSIM value. The second matrix then represents the spatial relationships between two regions in the range 10–20 km to calculate another SpSSIM value in the next bin (bin 2). When the bin series covers the whole region (bin *n*), the average of the SpSSIM values in each bin is calculated to denote the overall similarity between two OD matrices. As for SSIM, the SpSSIM value equals 1 when two OD matrices have the exact same pattern.

	D_1	D_2	-	-	-	D_n
O_1	0	20	129	30	180	202
O_2	24	0	0	2	0	0
.	76	1	0	15	0	8
.	26	6	1	0	5	0
.	101	2	0	4	0	101
O_n	122	0	7	3	194	0

	D_1	D_2	-	-	-	D_n
O_1	0	25	99	35	185	187
O_2	31	0	0	7	0	0
.	71	1	0	10	0	3
.	26	6	1	0	5	0
.	91	2	0	4	0	111
O_n	112	0	13	12	184	0

$w_{ij}^D = 0$

$w_{ij}^D = 1$

FIGURE 2 Comparison of two OD matrices using SpSSIM

$$\text{Global SpSSIM}\left(X,Y\right)=\frac{1}{n}\sum_{b=1}^{n}\text{SpSSIM}\left(X,Y,W^b\right) \tag{7}$$

Moreover, SpSSIM can compare local inbound flows (in-flows) and outbound flows (out-flows) (localized SpSSIM). The similarity of local directions of movement is measured by calculating SpSSIM with only columns or rows in a spatial weight matrix (Equation 8). When the *i*th rows of two matrices are compared in a geographic bin, the value of the localized SpSSIM represents the similarity of out-flows starting from the *i*th region. In contrast, the similarity of flows moving into the *j*th region can be calculated by comparing the *j*th columns of two matrices.

$$\text{Localized SpSSIM}\left(X,Y\right)=\begin{cases}\text{SpSSIM}\left(X_i,Y_i,W^b\right),\text{outflow}\\ \text{SpSSIM}\left(X_j,Y_j,W^b\right),\ \text{inflow}\end{cases} \tag{8}$$

3.2 | Bootstrap verification

To verify the statistical significance of SpSSIM, we employed bootstrapping to estimate the distribution. Bootstrapping generates a random distribution of a parameter by iteratively resampling the observed data (Westfall & Young, 1989). It simulates samples with the same size of observation and allows replacement (Efron, 1979). For example, with the set of observations $X=\{x_1,x_2,x_3,\ldots,x_n\}$, a sample can be $\tilde{X}_1=\{x_3,x_2,x_2,\ldots,x_n\}$. Then, the process of sampling is iterated a large number of times and the statistics of the created samples are computed. It is similar to Monte Carlo simulation regarding repeating a process, but Monte Carlo simulation generates random cases under a null hypothesis rather than resampling from the existing dataset. In this study, we resampled the observed amounts of flow from each OD matrix due to difficulties in assuming a null hypothesis for mobility patterns. We randomly resampled 999 times to generate the probability distribution of SpSSIM and estimates *p* values of the index based on the mean and standard deviation of resampled values. The *p* values verify whether the observed mobility patterns from two data sources are randomly different or not.

4 | DATA

4.1 | Building OD matrices from social media data

As a case study to demonstrate SpSSIM to measure similarity in human mobility, we compared OD matrices generated from three data sources, Twitter, Instagram, and LODES. First of all, we collected Twitter and Instagram geo-referenced posts using APIs from 12/07/2014 to 05/17/2015 (161 days) in San Diego County. To avoid duplicated

TABLE 2 Data summary

Source of social media	No. of posts originally collected	No. of posts after removing cross-platform data	No. of extracted daily movements
Twitter	2,202,719	1,916,580	116,253
Instagram	4,362,176	—	297,339

posts possibly generated by cross-posting from Instagram to Twitter, we considered tweets only posted from mobile-based Twitter application sources (e.g., Twitter for Android, Twitter for iPhone, etc.). This removed tweets cross-posted from other social media platforms, including Instagram and Foursquare. The numbers of posts in the period were 1,916,580 for Twitter and 4,362,176 for Instagram, respectively. From these social media posts, we extracted individual daily trip segments by connecting any two temporally adjacent geo-referenced points within the same day. For example, if a person posted a message on social media at location A in the morning and another at location B at night, then the segment from A to B is regarded as movement. If the person posts at three locations A, B, C sequentially in a day, the segment is regarded as two movements, A–B and B–C.

These extracted trip segments include irrelevant data such as no movements and movements with an unrealistically high velocity. To further clean up the irrelevant trip segments, we removed segments with zero distance where their origin and destination are at the same location. We also removed segments whose average velocity was greater than 65 miles per hour (mph), which is California's general maximum speed limit (California Department of Transportation, 2019). Then, we aggregated these trip segments to build OD matrices based on 41 San Diego SRAs as a spatial unit. SRAs represent local communities/neighborhoods that are suitable to describe regional contexts of human mobility. From the social media data, we extracted 116,253 and 297,339 individual daily movements between SRAs from Twitter and Instagram, respectively. Table 2 summarizes the number of data collected, processed, and generated for each social media platform.

To compare human mobility extracted from social media data with non-social media-based mobility data, we used the LODES data. It represents commuting patterns, or home-to-work flows, based on employer reporting records at census block level that can cover more than 90% of all employment categories except self-employment or military personnel (Horner & Schleith, 2012). We aggregated LODES flows into the SRA level to investigate the regional context of human mobility patterns. A flow between two SRAs was defined as f_{ij}, indicating that a person moved from the ith SRA to the jth SRA in a day. We define origin regions as rows and destination regions as columns in an OD matrix, where the sum of the ith rows denotes the total amount of out-flow from the ith SRA and the sum of the jth columns represents the total amount of in-flow to the jth SRA. To understand flows between neighborhoods, we removed internal flows whose origins and destinations are in the same region (f_{ii}). Then, we normalized the flows between SRAs through probability of flows, which scale the value of flows from all datasets to be between 0 and 1.

4.2 | Data description

Table 3 describes descriptive statistics of flows in three data sources. Generally, all probability distributions of flows were positively skewed. Almost all movements from three sources traveled within 50 km. Twitter and Instagram have more movements within 20 km (78.8 and 73.0%, respectively) than LODES (57.5%). However, LODES has the largest total amount of flows and the lowest percentage of zero cells, which refer to no movements between two SRAs. In LODES, there are 23 (1.4%) OD pairs of SRAs with no flow out of 1640 pairs (41 × 40), excluding internal flows. On the contrary, there are many OD pairs with no flow in Twitter and Instagram. It describes that the commuting-based mobility (LODES) was more ubiquitously distributed in San Diego County than social media-based mobility. This further indicates that social media was used more frequently within geographically confined regions rather than overall regions. Between Twitter and Instagram, Instagram-based flows (zero

TABLE 3 Descriptive statistics of flows

	LODES	Twitter	Instagram
Total amount	836,974	116,253	297,339
Mean	497.9	69.2	176.9
Median	91	8	14
Std. dev.	1,135.601	180.722	551.491
Max	10,438	1,539	7,163
1st quartile	19	2	0
3rd quartile	420	44	108
# of zero (ratio)	23 (1.4%)	219 (13.4%)	451 (27.5%)
Skewness	4.444	4.605	7.418
By 20 km	57.535%	78.849%	73.040%
By 50 km	96.490%	98.042%	98.116%

OD flows = 27.5%) were geographically sparser than Twitter-based flows (zero OD flows = 13.4%) even though the amount of flows in Instagram is 2.5 times more than that in Twitter. One potential explanation for these patterns is that each type of social media has different usages and purposes. For example, Twitter users are more likely to post messages at their ordinary locations such as home and work while Instagram users are more willing to share their extraordinary experiences by posting pictures at places of social activity and entertainment. Section 5 provides further discussions on the difference in flow between Twitter and Instagram.

Four maps in Figure 3 describe the density of total probability of flows in San Diego County and the spatial distributions of out-flows from LODES, Twitter, and Instagram, respectively. The majority of flows were concentrated in the western region of San Diego County, corresponding with the population distribution. Flows represented by an arrow in the maps are major flows, where the amount of flow is over 1.5 standard deviations from the mean of each source. To avoid over-cluttering, only flows larger than +1.5 standard deviations are displayed. The most frequent flows from LODES moved into two regions (highlighted by the yellow border in Figure 3a), Central San Diego—known as the Central Business District (CBD) of San Diego and Kearny Mesa—known as a new business district. Compared to LODES, flows from social media revealed that frequent destinations are not limited to those two business districts. Twitter users visited comparatively diverse destinations whereas Instagram users preferred traveling to coastal areas such as Coastal and Peninsula SRAs (Table 4).

5 | RESULTS

5.1 | SSIM and sensitivity

To test the sensitivity of the OD pairs ordering, we generated two sets of reordered OD matrices of each data source and compared the results of SSIM and SpSSIM. We resampled the orders of pairs twice based on: (a) the population size; and (b) the alphabetical order of the SRA name. For SSIM, we tested eight square windows, where the window size was increased from 5 to 40 cells in steps of 5 cells. For SpSSIM, we set 12 distance bins where the bin width is 10 km and the distance range is from 0 to 120 km. For each bin, we calculated SpSSIM using a spatial weights matrix determined by Equation (6). Cells of the nine heatmaps in Figure 4 represent the probabilities of movements, and rows and columns are origins and destinations, respectively. The LODES heatmaps illustrate an apparent tendency of central places to move within distinct lines whereas Twitter maps reveal relatively diverse patterns and Instagram maps look like mixed versions of the other two.

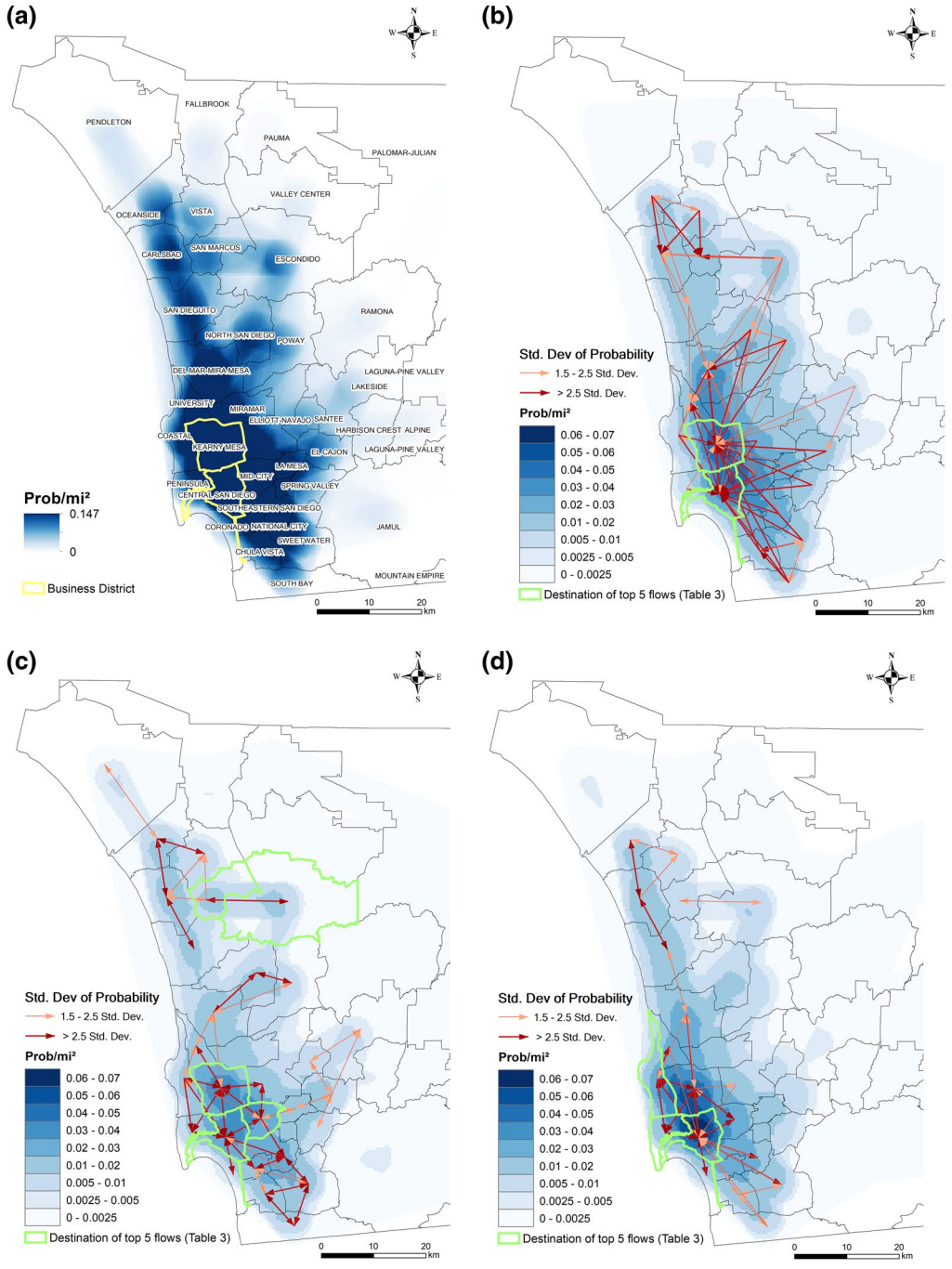

FIGURE 3 Spatial distribution of probability of flows: (a) total; (b) LODES; (c) Twitter; and (d) Instagram

We calculated SSIM by varying the sizes of windows to test the sensitivity of SSIM (Table 5). LODES and Twitter (L-T) have the lowest similarity while Twitter and Instagram (T-I) show similar patterns. However, the SSIM values differ by orders. For example, L-T have all different values of SSIM when the orders were shuffled, regardless of the window sizes. Reordered OD matrices basically represent the same phenomenon, but SSIM is incapable of identifying that they are the same patterns although the differences are slight. Moreover, SSIM fails to consider

TABLE 4 Top five flows between SRAs by data sources

	LODES		Twitter		Instagram	
Rank	Origin	Destination	Origin	Destination	Origin	Destination
1	Southeastern	Central	Central	Kearny Mesa	Coastal	Central
2	Kearny Mesa	Central	San Marcos	Escondido	Kearny Mesa	Central
3	Mid-City	Central	Kearny Mesa	Central	Central	Coastal
4	Central	Kearny Mesa	Kearny Mesa	Mid-City	Peninsula	Central
5	Del Mar-Mira Mesa	Kearny Mesa	Escondido	San Marcos	Central	Peninsula

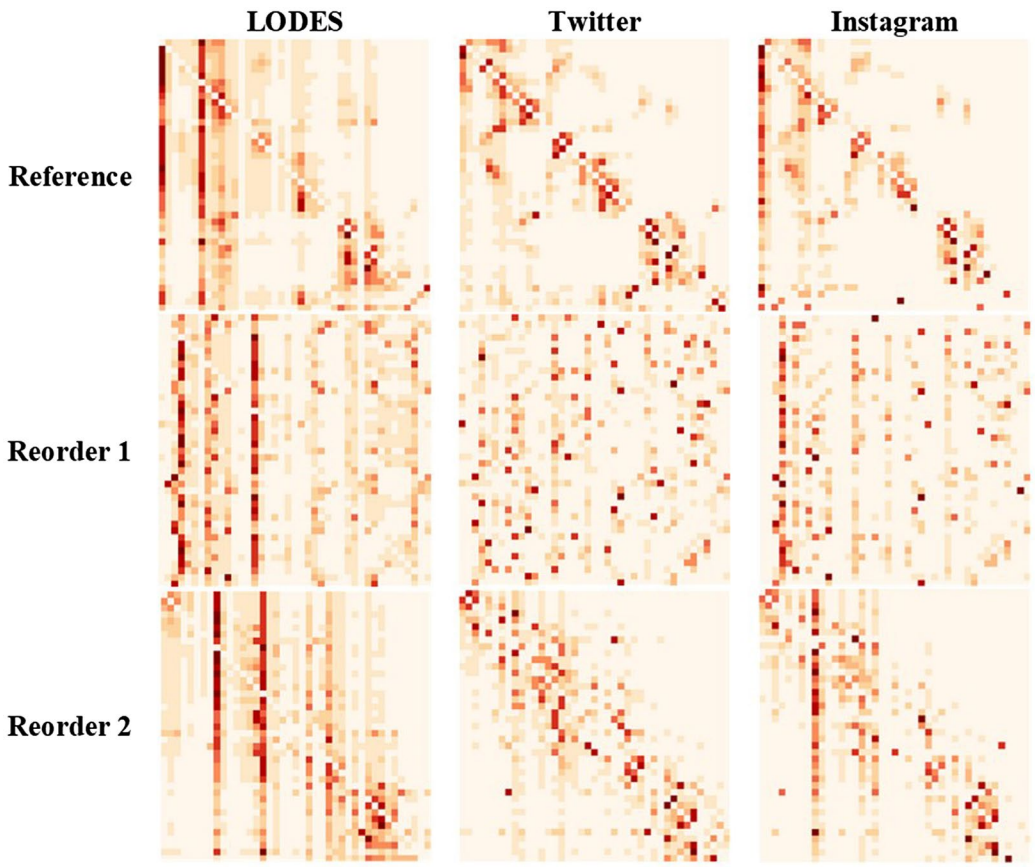

FIGURE 4 Heatmaps of OD pairs

spatial correlations between OD pairs. Since the two matrices were reordered by population and names, it is hard to guarantee that contiguous cells in a window are spatially close to each other. The sensitivity issues of pair ordering make SSIM less reliable, and it is challenging to define pair orderings.

Contrary to SSIM, SpSSIM produces the same value regardless of the order of OD pairs. Because the weight matrices in SpSSIM define the spatial relationships between SRAs, reordering does not affect the spatial arrangements of OD pairs whereas SSIM compares contiguous cells in OD matrices regardless of OD pairs' spatial configurations. Table 6 shows the SpSSIM values calculated for 12 travel distance bins. Most SpSSIM values up to 80 km travel distance range were significant at a 95% confidence level or better when compared to a random

TABLE 5 The values of SSIM by window sizes

OD		Window size							
		5	10	15	20	25	30	35	40
Reference	L–T	0.675	0.663	0.684	0.692	0.697	0.701	0.681	0.675
	L–I	0.715	0.729	0.754	0.758	0.760	0.743	0.703	0.668
	T–I	0.823	0.797	0.785	0.776	0.788	0.803	0.806	0.793
Reorder1	L–T	0.617	0.635	0.637	0.642	0.658	0.666	0.667	0.679
	L–I	0.682	0.692	0.694	0.692	0.683	0.670	0.650	0.644
	T–I	0.778	0.776	0.779	0.782	0.788	0.785	0.780	0.779
Reorder2	L–T	0.637	0.642	0.660	0.682	0.695	0.695	0.691	0.681
	L–I	0.687	0.676	0.658	0.646	0.636	0.632	0.630	0.644
	T–I	0.779	0.737	0.758	0.763	0.767	0.770	0.772	0.780

TABLE 6 The values of SpSSIM by spatial weight distances

	L–T			L–I			T–I		
D_{min}^{max} (km)	SpSSIM	Mean	Std. dev.	SpSSIM	Mean	Std.dev	SpSSIM	Mean	Std. dev.
0–10	0.655***	0.335	0.085	0.682**	0.371	0.113	0.841***	0.290	0.107
10–20	0.744***	0.257	0.054	0.680***	0.328	0.076	0.732***	0.205	0.064
20–30	0.467***	0.237	0.049	0.617***	0.318	0.069	0.793***	0.192	0.060
30–40	0.377*	0.252	0.052	0.610***	0.333	0.079	0.657***	0.206	0.066
40–50	0.466**	0.271	0.060	0.717***	0.344	0.087	0.623***	0.221	0.070
50–60	0.523***	0.285	0.062	0.704***	0.348	0.093	0.713***	0.228	0.073
60–70	0.520**	0.298	0.068	0.395	0.357	0.101	0.774***	0.251	0.085
70–80	0.594**	0.339	0.088	0.715**	0.377	0.117	0.878***	0.290	0.107
80–90	0.568	0.371	0.115	0.207	0.385	0.134	0.458	0.328	0.133
90–100	0.637	0.401	0.147	0.515	0.390	0.157	0.772*	0.371	0.157
100–110	0.753	0.419	0.246	0.000	0.411	0.257	0.000	0.406	0.251
110–120	0.000	0.425	0.316	0.000	0.392	0.328	0.000	0.000	0.000
Global	0.525**	0.344	0.018	0.487**	0.366	0.005	0.603***	0.249	0.098

***99.9%; **99%; and *95% significance level.

distribution. This demonstrates that the similarity between mobility patterns from each pair of sources is statistically significant. These results imply that SSIM is less suitable to be a measurement of similarity than SpSSIM because the former fails to calculate the same values from the same events while the latter succeeds.

5.2 | SpSSIM in San Diego County

The SpSSIM values in Table 6 represent the degree of similarity in the mobility patterns derived from two different data sources by distances. Overall, the mobility patterns between social media in San Diego County were more similar to each other (Global SpSSIM (T-I) = 0.603) than to LODES flows (Global SpSSIM (L-T) = 0.525; Global SpSSIM (L-I) = 0.487). The mobility similarity between LODES and Twitter is relatively higher under 20 km (0.655 and 0.744). It describes that Twitter users were more likely to make short trips, where origins and destinations were similar, to home and work locations reported in LODES in the travel distance range from 0 to 20 km. The

SpSSIM values, however, decrease steeply from 20 to 40 km (0.467 and 0.377). The dissimilarity increases since there are much fewer Twitter-based flows than LODES commuter-based flows in this distance range (Table 3). In addition, the majority of flows in LODES were heading to business districts such as Central San Diego and Kearny Mesa (see Figure 3b) while the destinations of Twitter users were diverse including beach areas (South Bay, Oceanside, and Del Mar-Mira Mesa) and parks (Sweetwater and Poway), as well as business districts (see Figure 3c). From 40 km, the SpSSIM value gradually increases again by 110 km since the probabilities in longer-distance trips were close to 0 for both data sources. Note that the SpSSIM values are not statistically significant over the range of 80 km. Compared to Twitter, mobility patterns from Instagram were less similar to those from LODES. Similar to other comparisons, the SpSSIM values of LODES and Instagram are relatively higher within 0 to 20 km. Unexpectedly, however, the similarity between LODES and Instagram peaked within 40 to 60 km. A potential explanation of this pattern is that the notable places in San Diego are concentrated in the downtown and coastal areas, where there are also many jobs. This similarity is also observed from Table 3 and Figures 3b and d. The most frequently visited destinations from two datasets are quite similar. It indicates that Instagram users are more willing to move longer distances than Twitter users if attractions are far away.

In contrast, travel patterns derived from Twitter and Instagram resemble each other. The SpSSIM value of Twitter and Instagram in the range of 0 to 10 km (0.841) is the highest in the same distance range bin and the second highest among all SpSSIM values. It explains that short daily trips observed from Twitter and Instagram users share similar origins and destinations, which are clustered in Central San Diego, Kearny Mesa, Peninsula, and Mid-City (Figures 3c and d). The SpSSIM values of Twitter and Instagram decreased slightly in the range of 10 to 20 km. Travel destinations of Twitter users in this distance range included suburban regions such as Escondido, San Marcos, Pendleton, and North San Diego whereas those of Instagram users were concentrated in the downtown regions of San Diego City such as Central San Diego, Coastal, and Peninsular. The SpSSIM values decreased further as the distance range increased to 30 to 50 km because the total probability of mobility derived from Twitter in the range (0.06) was smaller than that from Instagram (0.09). In addition, destinations of Twitter movements were more scattered than those of Instagram movements (Table 4).

5.3 | Localized SpSSIM

Localized SpSSIM helps investigate similarity in terms of local in-flows and out-flows. Figure 5 demonstrates an example of comparing localized in-flow SpSSIM between LODES and Twitter from 10 to 40 km. Since in-flows describe the number of people moving into a region, they represent the popularity of places. The mobility patterns from LODES and Twitter were less similar in Southeastern San Diego (highlighted by the blue border) within 20 km than other regions, indicating the lowest SpSSIM values in each range (0.074 and 0.120, respectively) while the global SpSSIM is the highest in the range 10–20 km (0.744). In contrast, the Del-Mar-Mira Mesa region (green border in Figure 5) showed different patterns. While the SpSSIM value was high in the range of 0 to 20 km, the value dropped from 30 km. In the range of 20 to 40 km, SpSSIM values were 0.289 and 0.181, respectively when the global values are 0.467 and 0.377. Although the dissimilarities were not as large as for Southeastern San Diego, they denote that the flows moving into the region changed dramatically from 30 km.

Figure 6 illustrates localized SpSSIM of the in-flows between Twitter and Instagram in the range of 0 to 40 km. Unlike the comparison of LODES and Twitter, most regions show relatively high values, indicating that Twitter and Instagram have similar mobility patterns. Within 10 km, the lowest localized SpSSIM value is 0.577 at the Southeastern San Diego SRA, denoting that the short-trip patterns of Twitter and Instagram users are relatively very similar. However, in the range of 10 to 20 km, Coastal (blue border in Figure 6, localized SpSSIM = 0.298) and Central San Diego (green border in Figure 6, localized SpSSIM = 0.404) display dissimilarity patterns compared to the global value in the range (0.732). This suggests that in-flow mobility patterns from two types of social media data in these two regions present notable dissimilarity when travel distances are 10–20 km (Figure 6b) or longer (Figures 6c and d).

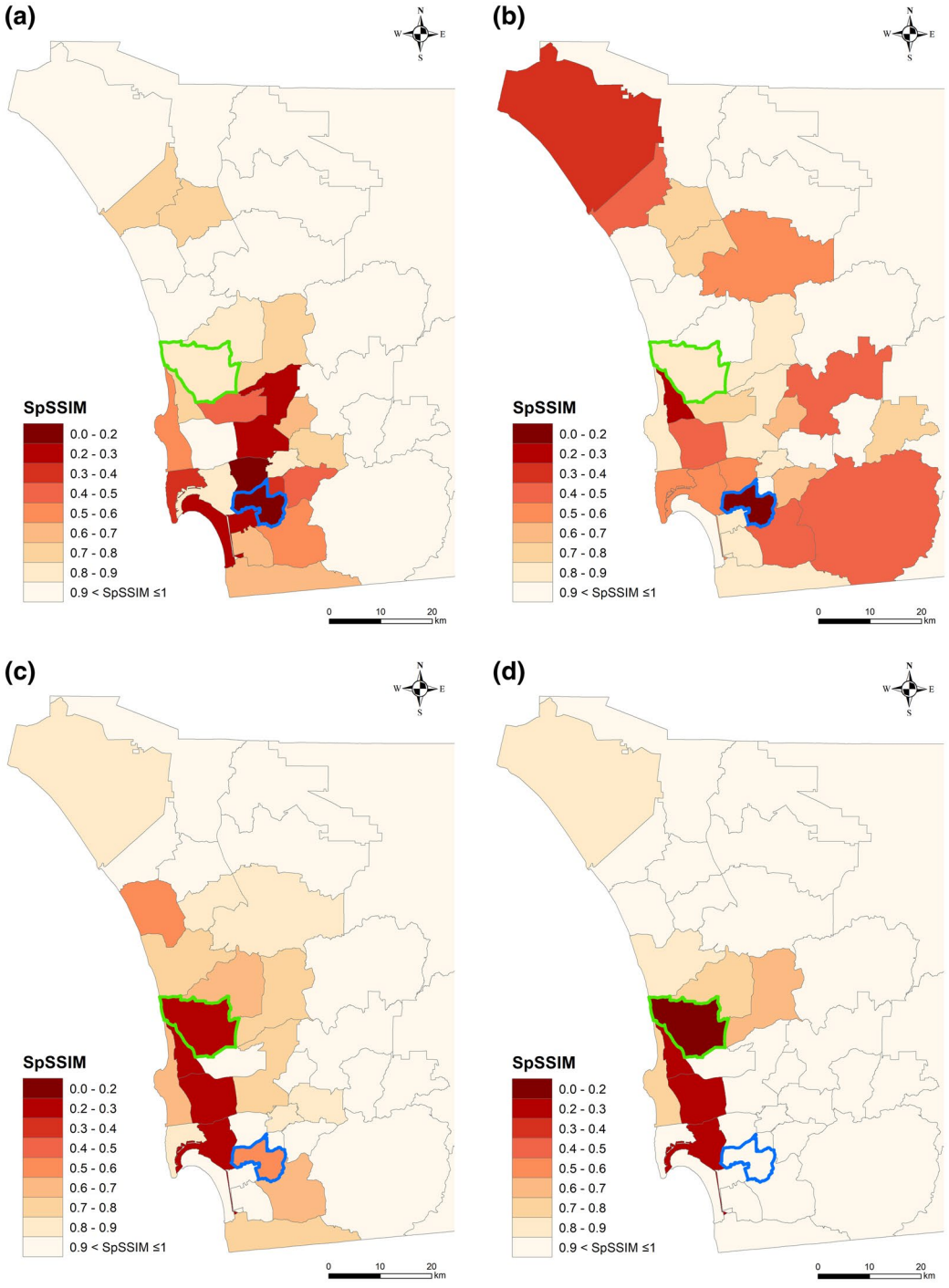

FIGURE 5 Localized SpSSIM (in-flows of L–T): (a) 10 km; (b) 20 km; (c) 30 km; and (d) 40 km

To further investigate the dissimilarity of the localized SpSSIM in these two regions, we mapped standardized differences of in-flows between two data sources by dividing the differences by the standard deviation of the difference. Figure 7a illustrates the standardized differences between LODES and Twitter regarding in-flows

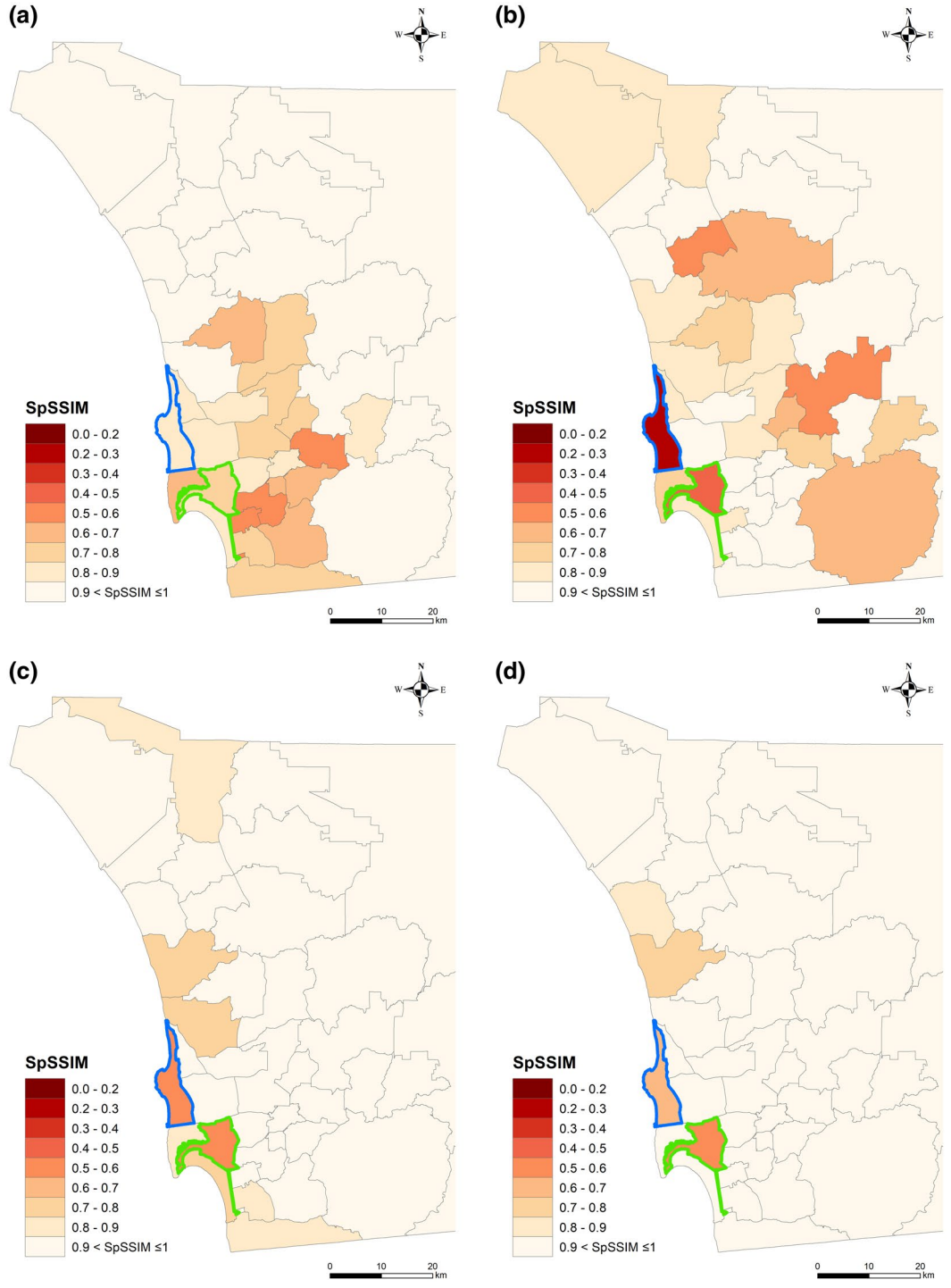

FIGURE 6 Localized SpSSIM (in-flows of T–I): (a) 10 km; (b) 20 km; (c) 30 km; and (d) 40 km

into the Southeastern San Diego SRA. The negative values in Figure 7a represent the probability that the movements derived from Twitter were larger than those from LODES. In other words, more Twitter users entered into Southeastern San Diego than LODES-based commuters within 20 km. In particular, the movements of Twitter

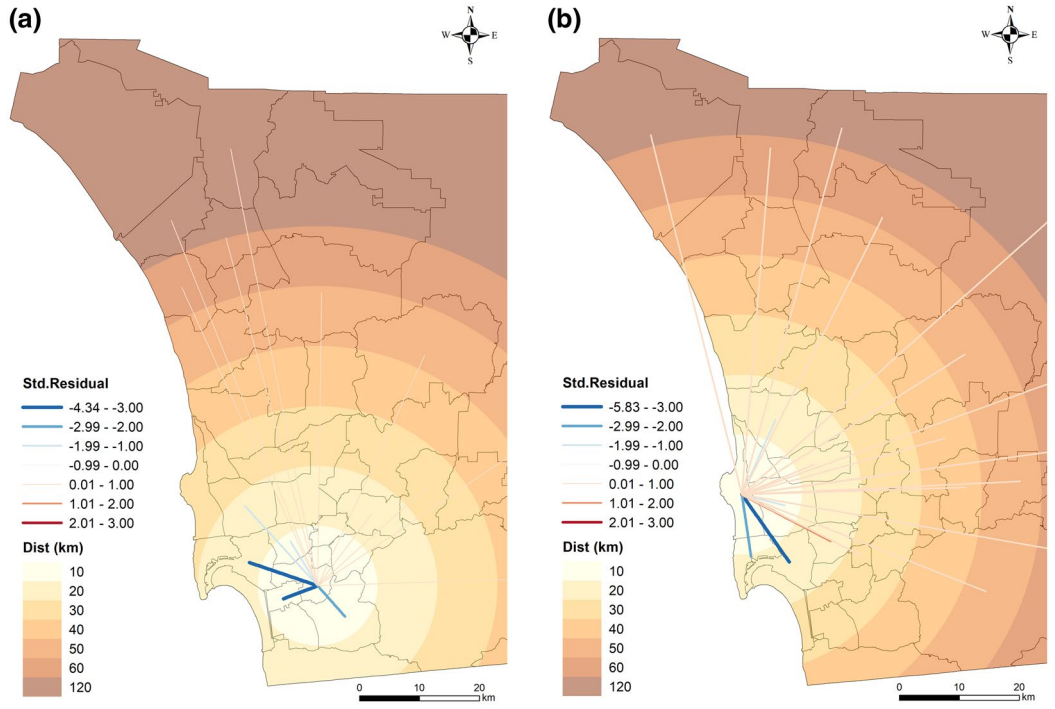

FIGURE 7 Standardized difference of in-flows: (a) Southeastern San Diego (LODES–Twitter); and (b) Coastal (Twitter–Instagram)

users between Central San Diego and National City, within 20 km from the origin, outnumbered the LODES movements. The localized SpSSIM detects the large differences with significantly low values (0.074 and 0.120). Similarly, Figure 7b demonstrates the differences between Twitter and Instagram flows moving into the Coastal SRA. Blue lines with negative values describe more Instagram users entering into the region than Twitter users. The localized SpSSIM also depicts a large inflow of Twitter users from the Mid-City to the Coastal SRA (orange line) when travel distances are within 20 km (local SpSSIM = 0.298), while most shorter-distance inflows to the Coastal SRA are dominated by Instagram users.

Although the localized SpSSIM values measure the differences between mobility patterns formed from OD matrices of diverse sources, the measurement itself does not provide the contexts behind the (dis)similarity. Here we provide potential explanations for the discovered patterns. Dissimilarities between LODES and Twitter in Southeastern San Diego (Figure 7a) can be explained by socioeconomic background. The Southeastern San Diego SRA has been one of the most impoverished areas in San Diego County (Joassart-Marcelli, Bosco, & Delgado, 2014). Due to its economic decline, there have been fewer job opportunities and places of attraction. Furthermore, the region has historically been more ethnically diverse than other areas. According to the American Community Survey 5-year (2007–2011) estimates, the Hispanic population made up over 50% of the total population, followed by the African and African-American population (18.2%). Due to lack of job opportunities in the region, LODES commuter-based in-flows were identified as low. In contrast, Twitter has been more popular among Hispanic African and African-American than other ethnic groups (Krogstad, 2015), which can explain the relatively large in-flows into the region by Twitter users.

The discovered patterns can also be described by the differences in social media platform usage. Gao (2015) and Steiger, Westerholt, Resch, and Zipf (2015) pointed out that tweets are most likely associated with home and workplace activities. Instagram, in contrast, has more geo-tagged pictures (18.8%) compared to Twitter (0.6%).

Since Twitter posts are more related to home and workplace activities, the similarity of LODES–Twitter is larger than that of LODES–Instagram (Table 6). Moreover, the dissimilarity of Twitter and Instagram in terms of in-flows into the Coastal SRA (Figure 6) can arise from the fact that there are many photogenic spots in the coastal region, where people are willing to share their experiences.

6 | CONCLUSIONS

In this research, we introduced a new method, SpSSIM, to measure the similarity between two OD matrices. We demonstrated the capability of SpSSIM by conducting a case study to compare three mobility data sources—LODES, Twitter, and Instagram—in San Diego County. In addition, we assessed the OD matrix ordering problem in SSIM when it is applied to spatial datasets. Our sensitivity test verified that SpSSIM is robust regardless of the arrangement of OD pairs while conventional SSIM is sensitive. This is achieved by employing a series of spatial weights matrices to resolve the sensitivity to the spatial configuration. SpSSIM is also verified statistically through bootstrapping, which generates the hypothetical distribution of SpSSIM values.

Our case study revealed notable similarities and differences in the mobility patterns from three data sources. In general, the mobility patterns of two social media types, Twitter and Instagram, resembled each other more so than when compared to LODES. The most frequent destinations of LODES were distributed in business districts while social media users were traveling to diverse points of interest. This is expected, since LODES flows are specifically comprised of employment-based home–work trips whereas Twitter and Instagram flows are based on social media users who have various purposes for their trips. SpSSIM can depict similarity over travel distances. For example, the similarity between LODES and Twitter increased in the range of 0 to 20 km and decreased steeply in the range of 20 to 40 km, which is explained by the sparseness of the mobility probability and the diversity of destinations in Twitter. Furthermore, SpSSIM can help discover local outliers by mapping localized values. We demonstrated in-flow (dis)similarities of LODES–Twitter and Twitter–Instagram. The localized SpSSIM values quantify and characterize the local mobility from different data sources by geographic distance.

While SpSSIM can successfully measure the similarity between two mobility datasets in the form of OD matrices, SpSSIM has two limitations. The first issue is that the distance ranges are defined arbitrarily and SpSSIM values are sensitive to them. SpSSIM utilizes a series of pre-defined distance bins to overcome the sensitivity of OD pairs and window sizes in SSIM. Further research is required to understand the sensitivity of defined distance bins. However, we argue that the use of the distance instead of the window size in SSIM can provide an explainable framework in terms of spatial context. Thus, SpSSIM helps measure the (dis)similarity of movements occurring in a specific spatial boundary in which researchers are interested. As another limitation, SpSSIM does not provide the amount of flow difference. Therefore, it is necessary to map the differences to understand the contexts of discovered mobility patterns (Figure 7). Nevertheless, SpSSIM, as an exploratory tool, provides spatial distribution of similarity with localized values and better understanding of the human dynamics and complexity in urban systems. By detecting outliers, researchers can selectively focus on investigating regions with high (dis)similarity and further study mobility contexts in those regions. In sum, this study provides a methodological approach to comparing mobility patterns in a spatial context and deepens our understanding of social media data in mobility analysis.

ACKNOWLEDGMENTS

This material is based on work supported by the National Science Foundation under Grant No. 1634641 (IMEE Project “Integrated Stage-Based Evacuation with Social Perception Analysis and Dynamic Population Estimation”). Any opinions, findings, and conclusions or recommendations expressed in this material are those of the authors and do not necessarily reflect the views of the National Science Foundation.

CONFLICT OF INTERESTS

The authors declare no potential conflicts of interest.

ORCID

Chanwoo Jin https://orcid.org/0000-0001-8883-8817
Atsushi Nara https://orcid.org/0000-0003-4173-7773
Jiue-An Yang https://orcid.org/0000-0003-4246-0470
Ming-Hsiang Tsou https://orcid.org/0000-0003-3421-486X

REFERENCES

Behara, K. N., Bhaskar, A., & Chung, A. B. E. (2017). Insights into geographical window based SSIM for comparison of OD matrices. In *Proceedings of the 39th Australasian Transport Research Forum*. Auckland, New Zealand.

Behara, K. N., Bhaskar, A., & Chung, A. B. E. (2018). Levenshtein distance for the structural comparison of OD matrices. In *Proceedings of the 40th Australasian Transport Research Forum*. Darwin, Northern Territory, Australia.

Brunet, D., Vrscay, E. R., & Wang, Z. (2012). On the mathematical properties of the structural similarity index. *IEEE Transactions on Image Processing*, *21*(4), 1488–1495.

California Department of Transportation. (2019). *California highways with 70 mph speed limits*. Retrieved from http://www.dot.ca.gov/hq/roadinfo/70mph.htm

Clayton, C. (1977). The structure of interstate and interregional migration: 1965–1970. *Annals of Regional Science*, *11*(1), 109–122.

Cresswell, T. (2012). *Geographic thought: A critical introduction*. Chichester, UK: John Wiley & Sons.

Crooks, A., Pfoser, D., Jenkins, A., Croitoru, A., Stefanidis, A., Smith, D., … Lamprianidis, G. (2015). Crowdsourcing urban form and function. *International Journal of Geographical Information Science*, *29*(5), 720–741.

Djukic, T. (2014). *Dynamic OD demand estimation and prediction for dynamic traffic management* (Unpublished PhD dissertation). Delft University of Technology, Delft, the Netherlands.

Dodge, S., Weibel, R., Ahearn, S. C., Buchin, M., & Miller, J. A. (2016). Analysis of movement data. *International Journal of Geographical Information Science*, *30*(5), 825–834.

Efron, B. (1979). Bootstrap methods: Another look at the jackknife. *Annals of Statistics*, *7*, 1–26.

Gao, S. (2015). Spatio-temporal analytics for exploring human mobility patterns and urban dynamics in the mobile age. *Spatial Cognition & Computation*, *15*(2), 86–114.

Gao, S., Janowicz, K., Montello, D. R., Hu, Y., Yang, J. A., McKenzie, G., … Yan, B. (2017). A data-synthesis-driven method for detecting and extracting vague cognitive regions. *International Journal of Geographical Information Science*, *31*(6), 1245–1271.

Gao, Y., Li, T., Wang, S., Jeong, M. H., & Soltani, K. (2018). A multidimensional spatial scan statistics approach to movement pattern comparison. *International Journal of Geographical Information Science*, *32*(7), 1304–1325.

Garrison, W. L., & Marble, D. F. (1964). Factor-analytic study of the connectivity of a transportation network. *Papers in Regional Science*, *12*(1), 231–238.

Greenwood, S., Perrin, A., & Duggan, M. (2016). *Social media update 2016*. Retrieved from http://www.pewinternet.org/2016/11/11/social-media-update-2016

Hawelka, B., Sitko, I., Beinat, E., Sobolevsky, S., Kazakopoulos, P., & Ratti, C. (2014). Geolocated Twitter as proxy for global mobility patterns. *Cartography & Geographic Information Science*, *41*(3), 260–271.

Horner, M. W., & Schleith, D. (2012). Analyzing temporal changes in land-use–transportation relationships: A LEHD-based approach. *Applied Geography*, *35*(1–2), 491–498.

Huang, Q., & Wong, D. W. S. (2016). Activity patterns, socioeconomic status and urban spatial structure: What can social media data tell us? *International Journal of Geographical Information Science*, *30*(9), 1873–1898.

Joassart-Marcelli, P., Bosco, F. J., & Delgado, E. (2014). *Southeastern San Diego's food landscape: Challenges and opportunities* (Policy Report). San Diego, CA: Department of Geography, San Diego State University and Project New Village.

Krogstad, J. M. (2015). *Social media preferences vary by race and ethnicity*. Retrieved from http://www.pewresearch.org/fact-tank/2015/02/03/social-media-preferencesvary-by-race-and-ethnicity/

Kulldorff, M. (1997). A spatial scan statistic. *Communications in Statistics*, *26*(6), 1481–1496.

Larsen, J., Urry, J., & Axhusen, K. (2006). *Mobilities, networks, geographies*. Farnham, UK: Ashgate.

Li, Z., Wang, C., Emrich, C. T., & Guo, D. (2018). A novel approach to leveraging social media for rapid flood mapping: A case study of the 2015 South Carolina floods. *Cartography & Geographic Information Science*, *45*(2), 97–110.

Liu, Y., Kang, C., Gao, S., Xiao, Y., & Tian, Y. (2012). Understanding intra-urban trip patterns from taxi trajectory data. *Journal of Geographical Systems*, *14*(4), 463–483.

Martín, Y., Li, Z., & Cutter, S. L. (2017). Leveraging Twitter to gauge evacuation compliance: Spatiotemporal analysis of Hurricane Matthew. *PLoS ONE*, *12*(7), e0181701.

Miller, H. J., & Shaw, S.-L. (2015). Geographic information systems for transportation in the 21st century. *Geography Compass*, *9*(4), 180–189.

Nara, A., Yang, X., Machiani, S. G., & Tsou, M.-H. (2017). An integrated evacuation decision support system framework with social perception analysis and dynamic population estimation. *International Journal of Disaster Risk Reduction*, *25*, 190–201.

Noulas, A., Scellato, S., Lambiotte, R., Pontil, M., & Mascolo, C. (2012). A tale of many cities: Universal patterns in human urban mobility. *PLoS ONE*, *7*(5), e37027.

Nystuen, J. D., & Dacey, M. F. (1961). A graph theory interpretation of nodal regions. *Papers of the Regional Science Association*, *7*(1), 29–42.

Panigutti, C., Tizzoni, M., Bajardi, P., Smoreda, Z., & Colizza, V. (2017). Assessing the use of mobile phone data to describe recurrent mobility patterns in spatial epidemic models. *Royal Society Open Science*, *4*, 160950.

Pearce, D. G. (1996). Domestic tourist travel in Sweden: A regional analysis. *Geografiska Annaler: Series B, Human Geography*, *78*(2), 71–84.

Pollard, T., Taylor, N., & van Vuren, T. (2013). Comparing the quality of OD matrices: In time and between data sources. In *Proceedings of the European Transport Conference*. Frankfurt, Germany: AET.

Poon, J., & Pandit, K. (1996). The geographic structure of cross-national trade flows and region states. *Regional Studies*, *30*(3), 273–285.

Salvador, S., & Chan, P. (2004). Determining the number of clusters/segments in hierarchical clustering/segmentation algorithms. In *Proceedings of the 16th IEEE International Conference on Tools with Artificial Intelligence* (pp. 576–584). Boca Raton, FL: IEEE.

Smith, H. T. R. (1970). Concepts and methods in commodity flow analysis. *Economic Geography*, *46*, 404–416.

Steiger, E., Westerholt, R., Resch, B., & Zipf, A. (2015). Twitter as an indicator for whereabouts of people? Correlating Twitter with UK census data. *Computers, Environment & Urban Systems*, *54*, 255–265.

Sun, Y., Fan, H., Li, M., & Zipf, A. (2015). Identifying the city center using human travel flows generated from location-based social networking data. *Environment & Planning B*, *43*(3), 480–498.

Wang, Q., & Taylor, J. E. (2014). Quantifying human mobility perturbation and resilience in hurricane sandy. *PLoS ONE*, *9*(11), e112608.

Wang, Z., Bovik, A. C., Sheikh, H. R., & Simmoncelli, E. P. (2004). Image quality assessment: From error visibility to structural similarity. *IEEE Transactions on Image Processing*, *13*(4), 600–612.

Wesolowski, A., Qureshi, T., Boni, M. F., Sundsøy, P. R., Johansson, M. A., Rasheed, S. B., … Buckee, C. O. (2015). Impact of human mobility on the emergence of dengue epidemics in Pakistan. *Proceedings of the National Academy of Sciences of the USA*, *112*(38), 11887–11892.

Westfall, P. H., & Young, S. S. (1989). P value adjustments for multiple tests in multivariate binomial models. *Journal of the American Statistical Association*, *84*, 780–786.

Wu, L., Zhi, Y., Sui, Z., & Liu, Y. (2014). Intra-urban human mobility and activity transition: Evidence from social media check-in data. *PLoS ONE*, *9*(5), e97010.

Xia, Y., Wang, G. Y., Zhang, X., Kim, G. B., & Bae, H. Y. (2011). Spatio-temporal similarity measure for network constrained trajectory data. *International Journal of Computational Intelligence Systems*, *4*(5), 1070–1079.

Xu, M., Li, Z., Shi, Y., Zhang, X., & Jiang, S. (2015). Evolution of regional inequality in the global shipping network. *Journal of Transport Geography*, *44*, 1–12.

Yuan, M., & Nara, A. (2015). Space-time analytics of tracks for the understanding of patterns of life. In M.-P. Kwan, D. Richardson, D. Wang, & C. Zhou (Eds.), *Space-time integration in geography and GIScience: Research frontiers in the US and China* (pp. 373–398). Berlin, Germany: Springer.

Yuan, Y., & Raubal, M. (2014). Measuring similarity of mobile phone user trajectories: A spatio-temporal edit distance method. *International Journal of Geographical Information Science*, *28*(3), 496–520.

Zheng, Y., & Zhou, X. (2011). *Computing with spatial trajectories*. New York, NY: Springer.

How to cite this article: Jin C, Nara A, Yang J-A, Tsou M-H. Similarity measurement on human mobility data with spatially weighted structural similarity index. *Transactions in GIS*. 2019;00:1–19. https://doi.org/10.1111/tgis.12590